

Received:
28 January 2018
Revised:
28 May 2018
Accepted:
8 August 2018

Cite as: A. Verde, O. Lastres, G. Hernández, G. Ibañez, L. Vereá, P. J. Sebastian. A new method for characterization of small capacity wind turbines with permanent magnet synchronous generator: An experimental study. *Heliyon* 4 (2018) e00732. doi: 10.1016/j.heliyon.2018.e00732



A new method for characterization of small capacity wind turbines with permanent magnet synchronous generator: An experimental study

A. Verde ^a, O. Lastres ^b, G. Hernández ^c, G. Ibañez ^b, L. Vereá ^b, P. J. Sebastian ^{a,*}

^a Instituto de Energías Renovables-UNAM, 62580, Temixco, Morelos, Mexico

^b Universidad de Ciencias y Artes de Chiapas, Ciudad Universitaria, Libramiento Norte Poniente 1150, 29039, Tuxtla Gutiérrez, Chiapas, Mexico

^c Universidad Popular de la Chontalpa, Cárdenas, Tabasco, Mexico

* Corresponding author.

E-mail address: sjp@ier.unam.mx (P.J. Sebastian).

Abstract

This work presents a new and useful method to dimension wind turbines and control systems and to optimize their mechanical design. This method allows determining the principal curves for characterizing a small capacity wind turbine designed with a Permanent Magnet Synchronous Generator (PMSG). For the wind turbine characterization it was considered the losses in the process of energy transformation in the wind rotor, electric generator and in the bridge rectifier. The equivalent electric model of the synchronous generator was used to determine the electric parameter performance. The work of the wind rotor was considered in its maximum power curve and the PMSG performance in the linear region of its magnetization curve. This leads to develop a new methodology for the complete wind turbine characterization from the nominal parameters of the wind rotor and the electric generator. This method also allows obtaining the power curves and the parameters of voltage, current and efficiency

around the wind speed domain and angular speed in the wind rotor. The method was tested for small-capacity wind turbine (1 kW and 10 kW) performances and the numerical and experimental results are described.

Keywords: Mechanical engineering, Energy

1. Introduction

The use of wind turbines in human activities has existed for more than hundreds of years. The environmental pollution due to fossil fuel use has promoted the development and application of this technology worldwide. Currently, there are wind turbines of different power capacity installed around the world. This work is focused on small capacity wind turbines (SCWT), which are generally designed for wind speeds of 10–15 [m.s⁻¹] [1].

The most common applications of the SCWT are in remote meteorological telemetry stations, in radio repeaters, in the energy supply system for rural areas, schools etc. They are also used as back up energy supply in systems where uninterrupted power supplies are required as in the petroleum extraction, refining and refueling for transportation and military outposts [2]. There is an important demand for SCWT of 1–10 kW that they are able to operate with several wind profiles. Some of these wind turbines are designed based on a Permanent Magnet Synchronous Generator (PMSG) and work with variable wind speed that optimizes the power generation [3, 4, 5, 6, 7, 8].

The variable speed operation of a wind turbine can be achieved with a Doubly Fed Induction Generator (DFIG) or with a PMSG. The PMSG has many advantages over the DFIG. The PMSG does not require DC excitation as the magnetic field is produced by the permanent magnets rather than by the coil. Hence, the PMSG does not require slip rings and brushes, which reduce the weight, cost, losses and maintenance [6, 7, 8, 9]. Another important characteristic of the PMSG is that the pole-slippage can be shorten which allows the use of a major number of poles and to eliminate the use of a gearbox to couple the rotor to the electric generator during the operation [10, 11, 12, 13].

The dimensioning of the wind turbine and its control system requires the knowledge of the static model to estimate the average loads to be supported by the mechanical structure of the wind turbine, the electric parameter behavior and the relation between the mechanical and the electrical parameters. Generally the synchronous generator model of outgoing poles is used [14, 15, 16, 17]. The analysis of the generator can be simplified when the magnets are mounted on the rotor surface of the generator and the machine can be considered as smooth poles with a high air gap resulting in the same inductance of armature reaction as in the direct and quadrature axes [18, 19, 20].

The models of magnetic and electrical circuits are used typically in the design, analysis and simulation of electric generator [10, 11]. The density of magnetic field is homogeneous in the mathematical model of PMSG, which simplifies the analysis and allows the use of these models for different design frequencies.

Some studies about wind turbines with PMSG have been reported and the losses in the air gap and the mechanical components were neglected [21, 22, 23]. However, in the framework of a PMSG these losses could be from 10 to 20% of the total losses in the system, which might represent a significant error in the estimation of the characteristic curves of the system [24]. There are some PMSG models reported for SCWT where the fixed losses in the generator are neglected [25, 26, 27]. There are also studies of the wind turbine performances related to the rotor design attending the wind conditions but without considering the electric generator [28, 29, 30, 31, 32]. Some other studies have reported the coupling of the rotor and the generator drive shaft considering the mechanical losses due to the bearings with the aim of determining the minimum wind speed for the starting of the generator [33]. Then, the losses, which are not considered from all other components of the wind system could be the reason that explains the differences between the theoretical power curve and the real power curve measured in a commercial wind turbine, as reported by Ciaran et al. [34]. Matteo et al. [35] reported a study of the PMSG connected to a three-phase bridge rectifier to evaluate the efficiency of the PMSG, the iron losses are approximated by the no load iron losses and the mechanical losses are also considered. This work does not consider the coupling of the PMSG with a wind rotor or the complete system [35].

This work describes the development of a new methodology to obtain the characteristic curves from $v_i = 0$ to $v_i = v_n$ of small capacity wind turbines with variable speed based on permanent magnet synchronous generator that can be considered as smooth. One of the major advantages of this method is that it includes the fixed losses in the generator and only requires a minimum number of electrical design parameters of the wind turbine to be used. The results can also be used to program the maximum power curve in a grid tie inverter or battery charger converter for stand-alone systems or to connect a water pump directly to the converter. The model considers the output power and rotor rotational speed having constant values when the wind speed (v_i) is higher than the nominal speed (v_n) and lower than the cutting speed (v_{cut}), these conditions are achieved through a control system of the wind turbine and not considering the inertia. Finally, this methodology is applicable for wind turbines of small, medium and high capacities as long as they are designed with PMSG.

2. Model

The mechanism of the power conversion generally applied in a small capacity wind turbine with a PMSG consists of a direct coupling of the wind rotor with the generator as illustrated by Fig. 1.

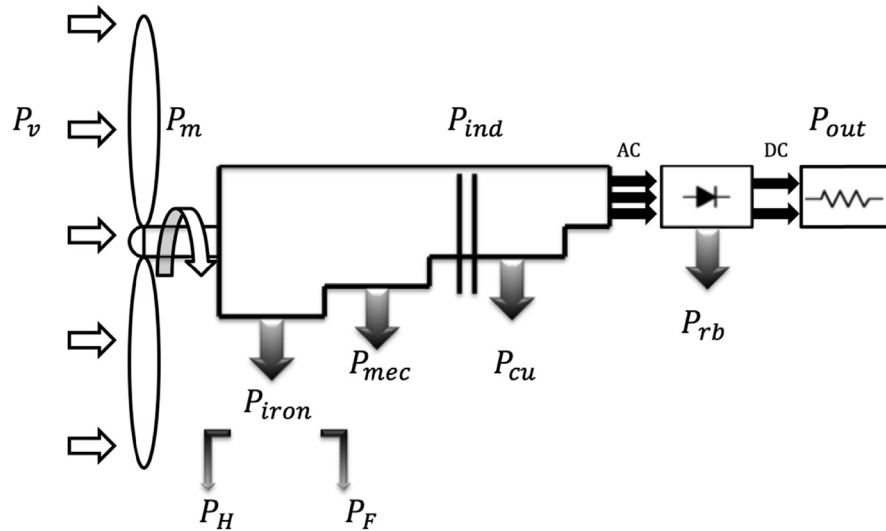


Fig. 1. The block diagram of the wind energy conversion model.

This diagram shows how the wind power P_v is converted in mechanical power P_m through the wind rotor due to the aerodynamic effect of the blades. The driveshaft is directly coupled to the generator to convert the mechanical power in electrical energy through the electromagnetic induction generated by the movement of a set of coils in the magnetic field [11]. In the power conversion process, the losses of the system are located in the iron rotor (hysteresis loss and Foucault loss), and there are also mechanical losses and copper losses due to Joule effect in the wind rotor [36].

The basic principles are described below to establish an equation that relates the fixed losses of the PMSG with the rotational speed of the rotor to obtain the wind turbine characteristic curves. The wind turbine power curves are determined for an optimum tip speed ratio (TSR) that ensures the maximum energy extraction from the rotor. The model initiates with the maximum mechanical power obtained from the wind rotor represented as follows [37]:

$$P_m = 0.5\rho Av^3 C_{pmax} = T_m \omega_m \tag{1}$$

where ρ is the air density, A is the area of the wind rotor and v is the wind speed, T_m is the mechanical torque and ω_m is the rotational speed. TSR is defined as the ratio of the speed at the tip of the blade and the wind speed as Eq. (2) [38]:

$$\lambda_0 = r_m \omega_m / v \tag{2}$$

The mechanical torque for C_{pmax} delivered for the wind rotor is proportional to the rotational speed of the turbine (rad/s) and it is described by the Eq. (3) [18].

$$T_m = P_m / \omega_m = (1/2\lambda_0^3) \rho \pi R^5 C_{pmax} \omega_m^2 = c \omega_m^2 \tag{3}$$

where c is a constant.

The wind turbine has a synchronous generator and hence the electrical frequency produced is synchronized with the rotational speed of the generator as: [10].

$$f_e = \omega_m P / 4\pi \tag{4}$$

where f_e is the electrical frequency and P is the number of poles.

The induced power in the stator of the three-phase electric generator can be expressed, considering the mechanical power in the driveshaft through the iron and mechanical losses due to electrical power produced and copper losses, as follows [11]:

$$P_{ind} = T_{ind}\omega_m = NE_a I_a \cos\Psi = NV_a I_a \cos\phi + P_{cu} \tag{5}$$

$$P_{ind} = P_m - P_h - P_{mec} \tag{6}$$

The induced mechanical torque is represented as:

$$T_{ind} = P_{ind} / \omega_m \tag{7}$$

The iron losses of the stator in a synchronous generator can be expressed as [11, 39]:

$$P_h = P_H + P_F = (k_H f_e B_m^\infty + k_F f_e^2 B_m^2 a^2 \sigma) \cdot vol \tag{8}$$

For PMSG, the B_m , k_H , k_F , a^2 and σ are constants and ω_m is directly proportional to f_e (Eq. (4)) then the iron losses can be represented as:

$$P_h = k_a f_e + k_b f_e^2 = A\omega_m + B\omega_m^2 \tag{9}$$

The mechanical losses are described in Eq. (10) [9]:

$$P_{mec} = C\omega_m + D\omega_m^3 \tag{10}$$

where C describes the mechanical losses due to friction and D the ventilation losses. From Eqs. (9) and (10) and neglecting the ventilation losses (because the fan is not required in this kind of machine) the total losses (P_{per}) in the wind turbine are expressed as

$$P_{per} = P_h + P_{mec} = k_1\omega_m + k_2\omega_m^2 \tag{11}$$

where $k_1 = A + C$ and $k_2 = B$, and

$$P_{per} = T_{per}\omega_m \tag{12}$$

from Eqs. (11) and (12) it can be simplified as:

$$T_{per} = k_1 + k_2\omega_m \tag{13}$$

In particular conditions when $\omega_m = 0$ and $k_1 = T_{min}$

$$T_{per} = T_{min} + k_2\omega_m \tag{14}$$

where $k_2 = (T_{per} - T_{min})/\omega_m$ and this can also be obtained from the nominal parameters of the PMSG.

Finally, the rotational speed of the rotor is related with the fixed total losses and Eq. (15) is obtained.

$$P_{per} = T_{min}\omega_m + k_2\omega_m^2 \tag{15}$$

The electrical power is obtained by the electrical analysis of the equivalent circuit of the one phase of the PMSG (Fig. 2). The mathematical model of the system is represented according to Eq. (16).

$$E_a = V_a + R_a I_a + jX_s I_a \tag{16}$$

The electrical circuit in Fig. 2 can be represented as a phasor diagram (Fig. 3), to show the relationship between the phase voltage (V_a) and the power factor. Eq. (17) shows the mathematical expression of the angles from the phasor diagram.

$$\psi = \varphi + \delta \tag{17}$$

To obtain an approximation of the output power of the generator, the resistance in the armature is considered negligible (See Fig. 4) and E_a and I_a can be expressed as:

$$I_a X_s \cos\varphi = E_a \sin\delta = x \tag{18}$$

The electromotive force (EMF) induced in the stator of the synchronous generator is obtained as [11]:

$$E_a = K\phi\omega_m \tag{19}$$

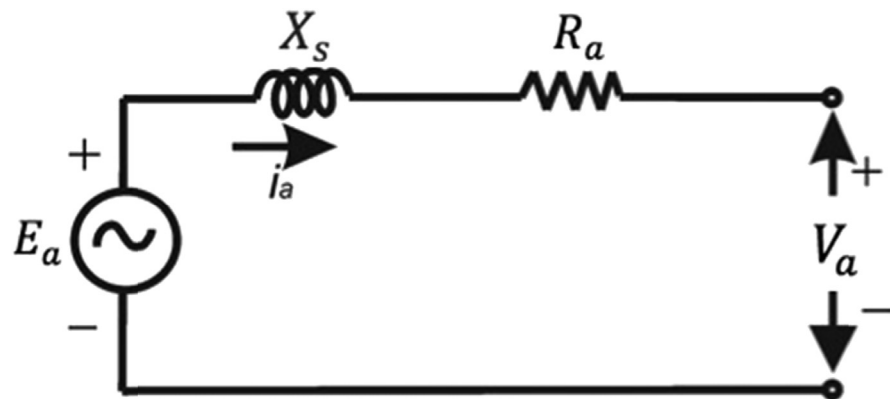


Fig. 2. The electrical circuit of the one phase of the PMSG [10].

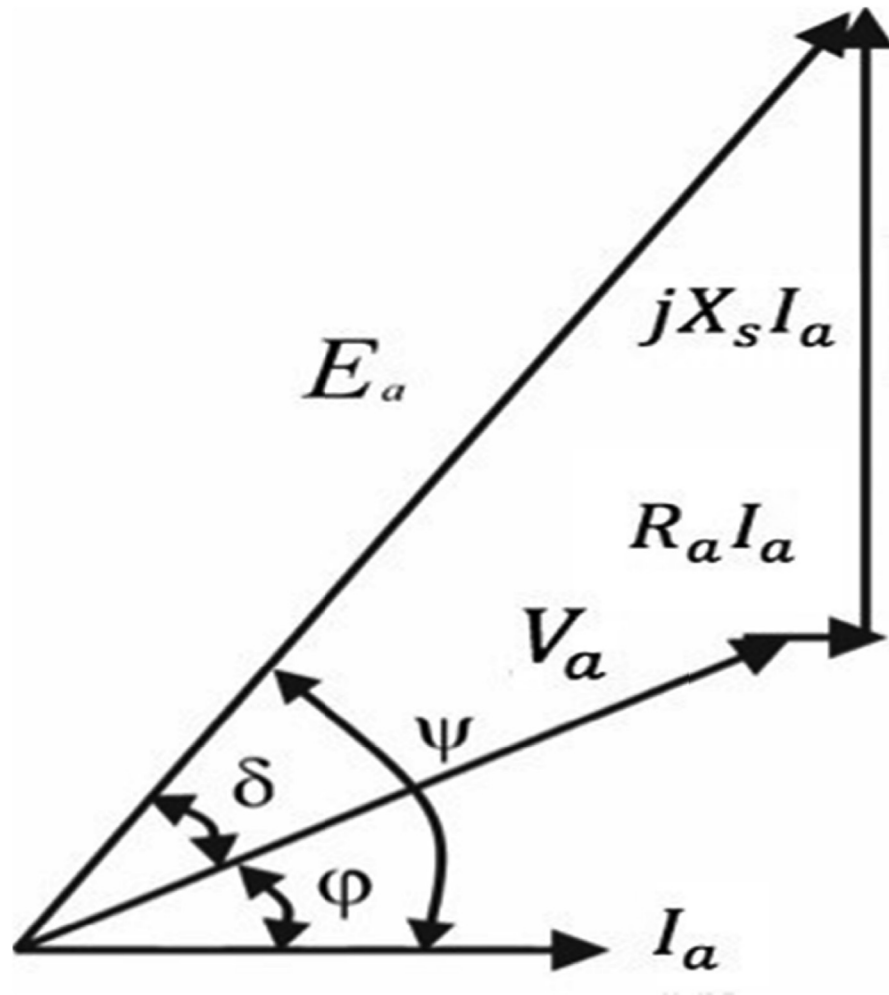


Fig. 3. The phasor diagram of the one phase synchronous generator [10].

where K is a constant that includes the number of poles and the number of turns in each winding and ϕ is the magnetic flux. For permanent magnet generators the ϕ can be consider as a constant parameter, resulting in the following expression.

$$E_a = K_E \omega_m \quad (20)$$

where K_E represents the new constant.

The phase current in a PMSG can be expressed as:

$$I_a = T_{ind} \omega_m / N E_a \cos \Psi \quad (21)$$

The copper losses are represented as:

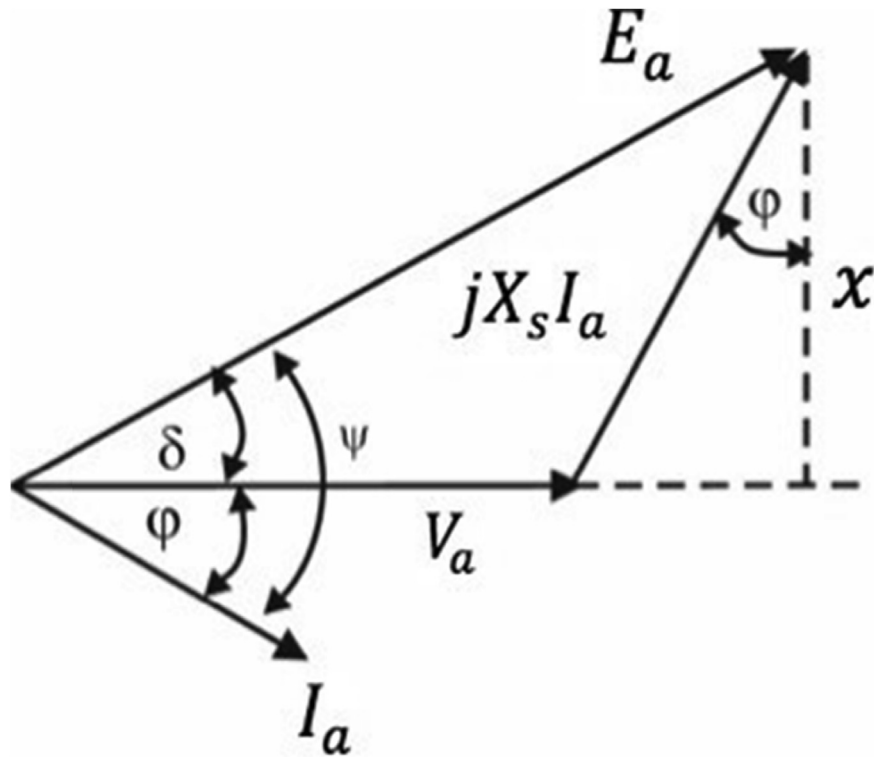


Fig. 4. The simplified phasor diagram of the one phase synchronous generator [10].

$$P_{cu} = NI_a^2 R_a \tag{22}$$

where R_a is the electric resistance of the one phase.

The electrical power of the generator is defined by Eqs. (23), (24), and (25) [10].

$$P_{act} = NV_a I_a \cos\phi \tag{23}$$

$$P_{rea} = NV_a I_a \sin\phi \tag{24}$$

$$P_a = NV_a I_a \tag{25}$$

The PMSG is located before a three-phase rectifier bridge to convert the alternate current to direct current. The Eqs. (26) and (27) describe the three-phase rectifier bridge [18].

$$V_{dc} = (0.95/\pi) (3\sqrt{2}) V_a \tag{26}$$

$$I_{dc} = P_{act}/V_{dc} \tag{27}$$

3. Methodology

This methodology is presented as a block diagram as shown in Fig. 5 where it is described the process to obtain the characteristic curves of a wind turbine from the wind speed or the rotor rotational speed.

The complete methodology can be simulated considering four stages:

- Stage 1. Determination of the wind rotor parameters.

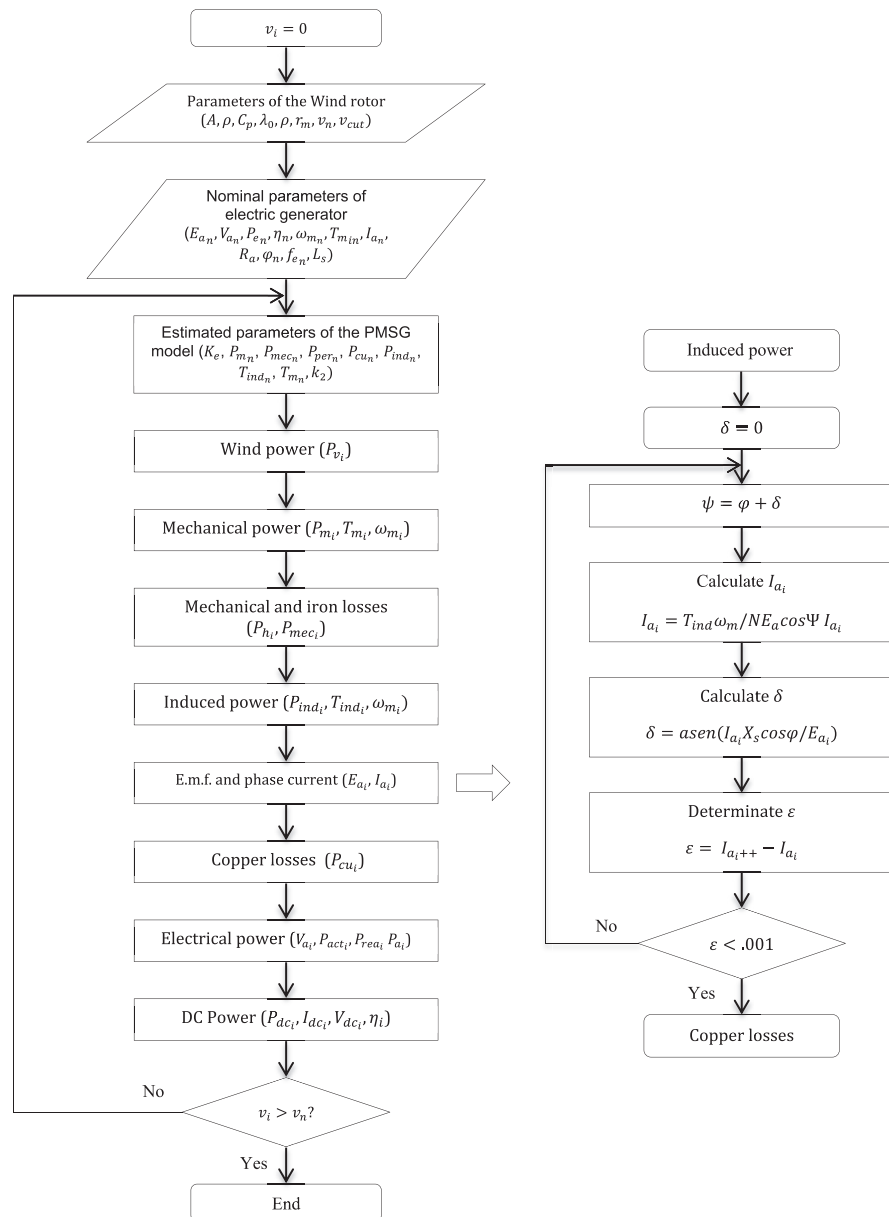


Fig. 5. The block diagram of the methodology developed for PMSG characterization.

The parameters considered for the methodology of the wind turbine are:

Power coefficient (C_{pmax}), optimum TSR (λ_0), air density (ρ [kg m^{-3}]), the rotor radius (r_m [m]) and the nominal wind speed (v_n [m s^{-1}]).

- Stage 2. Determination of the nominal parameters of the electric generator.

The nominal parameters of electric generator required to apply them in the model are:

The e.m.f. (E_{an} [V]), phase voltage (V_{an} [V]), electrical power (P_{en} [W]), frequency (f_{en} [Hz]), efficiency (η_n), rotational speed (ω_{m_n} [rad s^{-1}]), phase current (I_{an} [A]) starting mechanical torque (T_{min} [Nm]), phase resistance (R_a [Ω]) the angle of lag (φ_n) and the inductance (L_s [H]).

- Stage 3. Estimating the parameters of the PMSG.

The nominal parameters of the PMSG required for the model (see Fig. 5) can be obtained from the data sheet given by the manufacturer or measured in a test bench. These data are introduced in the equations presented in the wind energy conversion model as:

The constant K_e obtained with the EMF_n and the nominal rotational speed (ω_{m_n}). The nominal mechanical power (P_{m_n} [W]) calculated with the nominal electric power (P_{en}) and the nominal efficiency. The nominal copper loss power (P_{cu_n} [W]) obtained from Eq. (22) with the nominal phase current I_{an} . The nominal induced power (P_{ind_n} [W]) calculated with the nominal active power and the nominal copper losses. The nominal total losses Power (P_{per_n} [W]), obtained from the difference between the nominal induced power and the nominal mechanical power. The constant K_2 obtained with the Eq. (15), P_{per_n} and ω_{m_n} .

- Stage 4. Applying the model.

The constants obtained in the previous stage determine the fixed losses of the electric generator. Then the model is applied to obtain the characteristic curves of the wind turbine from $v_i = 0$ to $v_i = v_n$.

4. Results and discussion

The methodology developed in this work was successfully employed to measure the electrical parameters and to validate the numerical results (Fig. 7) obtained from a 1 kW wind turbine manufactured by RTO Energy (Fig. 6) with Direct Driver model of PMSG.

The results obtained from the wind turbine operation are presented as a function of the rotational speed due to the considerations made for the model and the initial



Fig. 6. 1 kW wind turbine manufactured by RTO Energy company.

conditions of the system. The methodology described in Fig. 5 was employed to characterize the electrical generator connected to a three-phase rectifier bridge, which was connected to a resistive charge (Fig. 7).

The input parameters of the system considered were the mechanical power (P_m) and the rotational speed (ω_m). The output parameters of the electrical generator were the phase voltage (V_a), the phase current (I_a), e.m.f. (E_a) and the active power (P_{act}). The voltage (V_{dc}) and the electrical current (I_{dc}) were measured in the rectifier bridge.

The theoretical and the experimental behaviors of the basic parameters are shown below, from Figs. 8, 9, 10, and 11. The input parameters of the methodology are considered in the mechanical power curve versus mechanical speed shown in

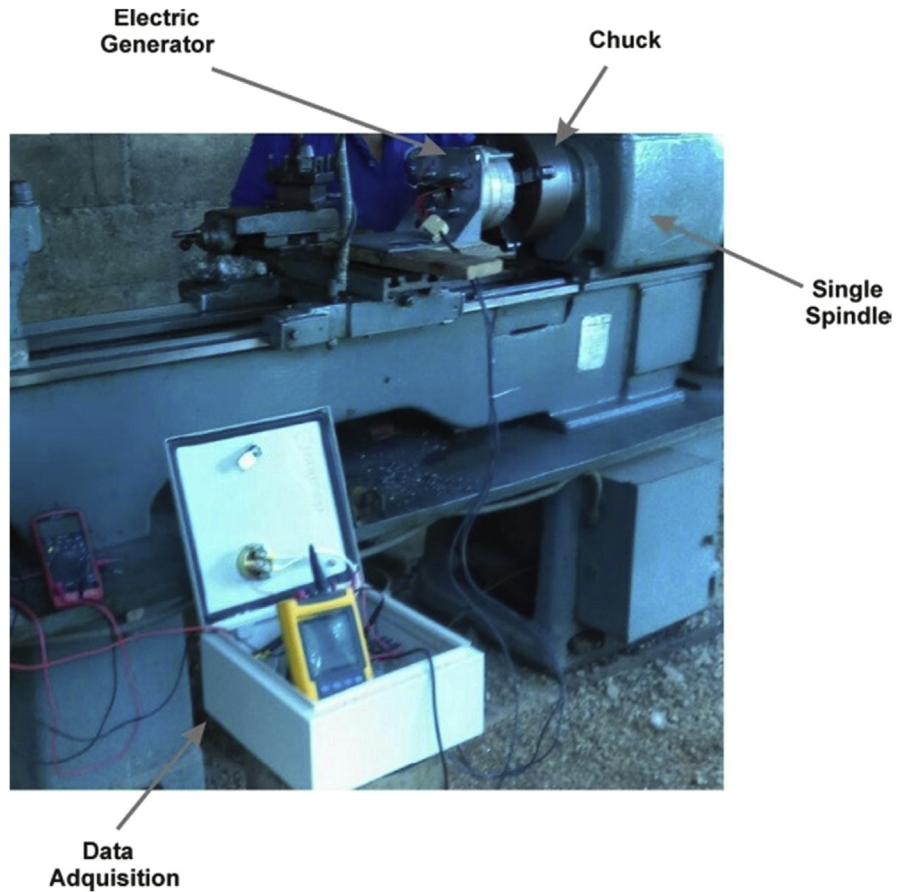


Fig. 7. Test experimental Electrical Generator.

Fig. 8. The validation of the theoretical and experimental results is presented as the active power curves represented as P_{act_t} and P_{act_e} in the PMSG output.

This figure also demonstrate that the variation from the experimental and the theoretical power in direct current (P_{dc_t} and P_{dc_e}) was 5.2% at the start and as the power

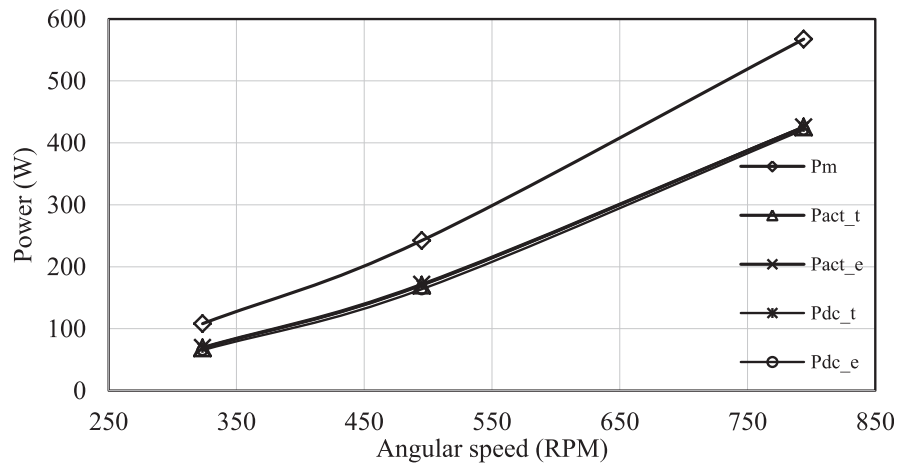


Fig. 8. Comparison of the theoretical and the experimental results of the active power and the DC power.

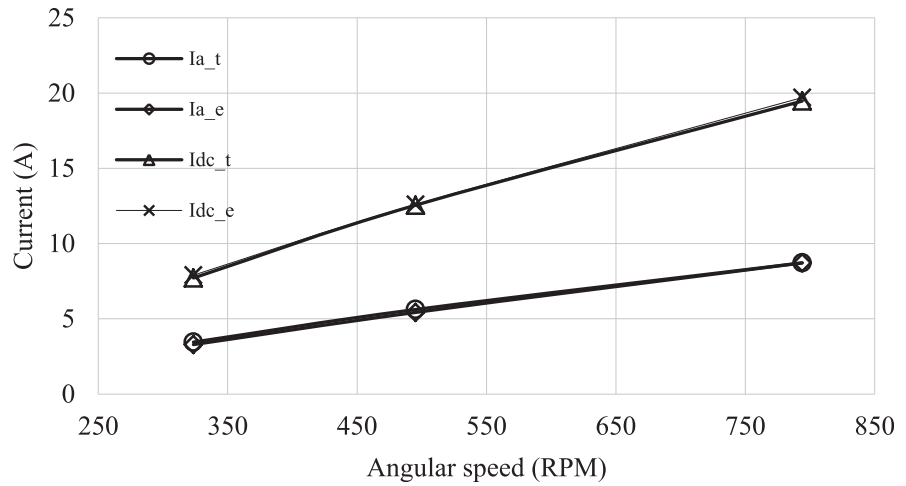


Fig. 9. Comparison of the theoretical and the experimental results of phase current and DC-bus current.

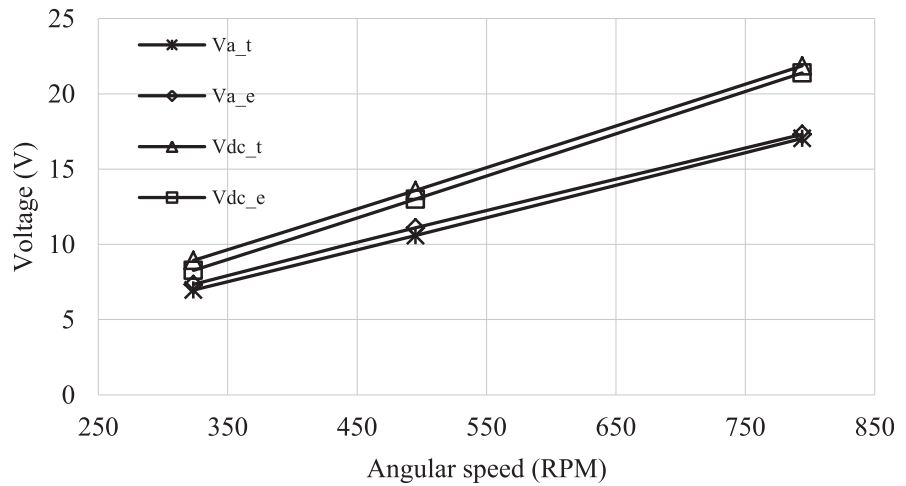


Fig. 10. Comparison of the theoretical and the experimental results of phase voltage and DC-bus voltage.

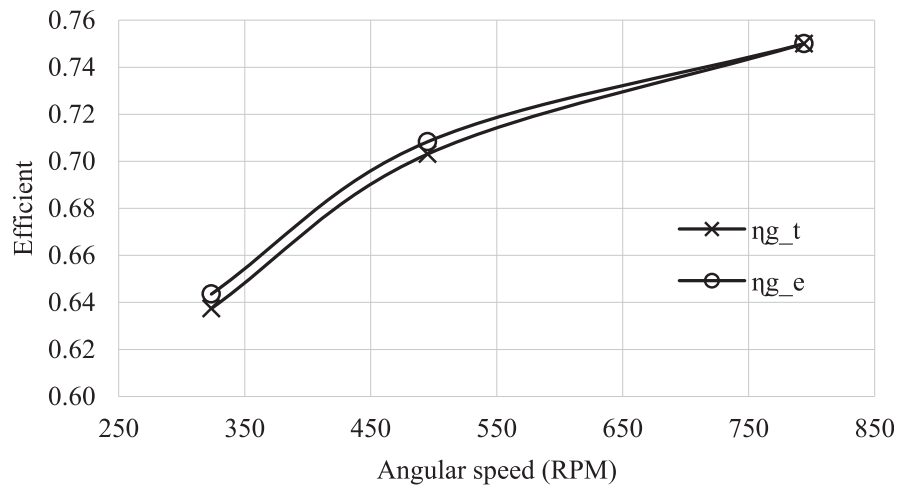


Fig. 11. Efficiency analysis of the electrical generator.

increased to the maximum mechanical speed tested the variation decreased to 1%. The losses in the mechanical power were estimated as 6.6% and 8% due to the losses in the copper wires. As it was expected the losses increased with the rotational speed because they are proportional to the current. The losses due to the iron were also considered and they represented 30% in the start and decreased to 17% at nominal speed.

The comparison of the theoretical and the experimental phase currents I_{a-t} and I_{a-e} respectively and the output currents of the rectifier bridge I_{dc-t} and I_{dc-e} are shown in Fig. 9. The linear behavior of the current is due to the fixed value of the resistive load. The typical error between the theoretical and the experimental values of the phase current is 8% and the DC-bus current is 12%.

The experimental and the theoretical values of the phase voltage in the PMSG outlet and the Rectifier Bridge outlet voltage are shown in Fig. 10. The variation from the theoretical to the experimental results were estimated as 5.1% in the PMSG output at 323 RPM and it was observed a decrease until 1.6% as the rotational speed increases to 794 RPM. The maximum difference of 7.4% between the experimental and theoretical output voltage in the rectifier bridge was observed with the initial conditions and decreased until 2.2% in the maximum mechanical speed.

The results of the PMSG efficiency shown in Fig. 11 prove the effectiveness of the methodology described in this work because the theoretical and the experimental values obtained for low mechanical speed and nominal speed are practically the same.

The methodology developed here shows and also proves the importance of considering the losses due to the material (iron and copper) and to the mechanical properties. The total losses of the wind turbine were estimated from 40% to 26% as the power generation increased. When these losses are not considered the error in the measurement of the power would be from 30% to 17%. For example, the maximum efficiency of the electric generator in this work was 75% at 795 RPM and without considering the losses the efficiency estimated would be more than 90% and then the energy coupling is compromised. These analyses prove the importance of the loss quantification in low power wind turbines.

4.1. Case study: wind turbine of 10 kW

An electric generator of 10 kW was also studied with the methodology developed in this work. For this case the nominal data were obtained from the information provided by the PRECILEC Company and they are summarized in Table 1. This information was used to determine the characteristic curve of the wind turbine (Table 2). These data could also be obtained from a test bench.

The values of the parameters in Tables 1 and 2 were used for a simulation with a tool developed in Matlab/Simulink®. The wind speed considered was from 0 to 25 $\text{m}\cdot\text{s}^{-1}$. The numerical response of the system is shown in the following figures.

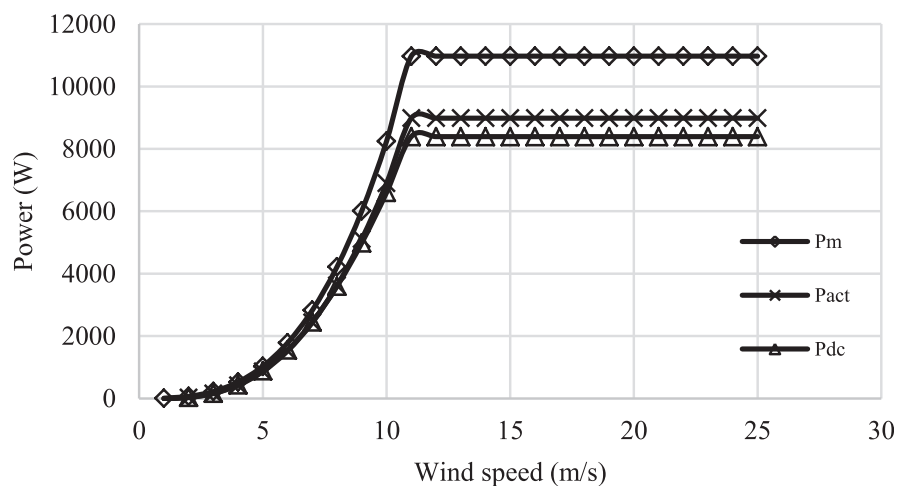
Table 1. Nominal parameters of the PMSG.

Parameter	Symbol	Value
Line voltage	V_L	240 V
Apparent power	P_a	10 kVA
Line current	I_L	24 A
Power factor	PF	1
Efficiency	η	>92 %
Angular speed	ω_m	210 RPM
Frequency	f	56 Hz
Torque	$T_{m_{in}}$	6.8 Nm
Phase resistance	R_a	0.27 Ω
Connection		Y

Table 2. Characteristics of the wind rotor.

Parameter	Symbol	Value
Radius	r_m	3.3 m
Optimal TSR	λ_0	6.6
Power coefficient	C_p	0.4
Nominal wind speed	v_n	11 m/s

The performance of the mechanical power P_m , the output active power of generator P_{act} , and the output power of the rectifier bridge P_{dc} related with the wind speed considered for the simulation are shown in Fig. 12. It was observed that the losses of the mechanical power in the electric generator are 18.12% at nominal speed and 6.6% of the active power in the bridge rectifier.

**Fig. 12.** Mechanical, active and DC power of the 10 kW wind turbine.

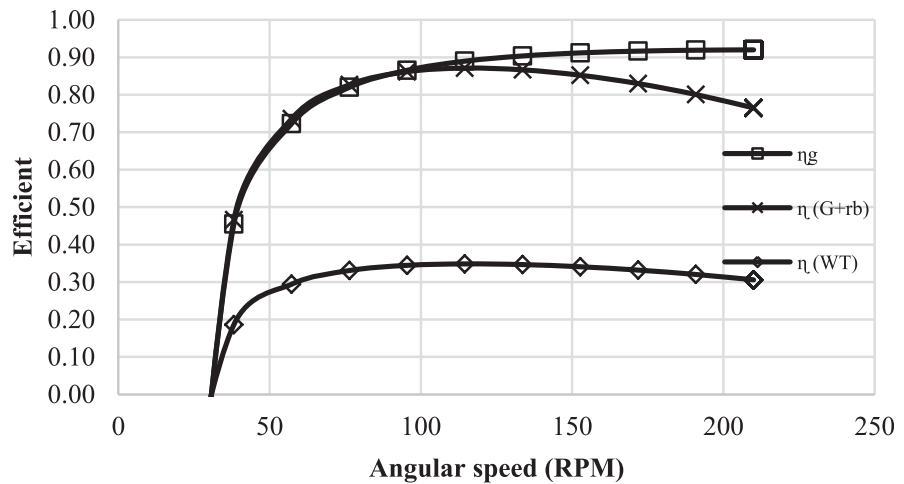


Fig. 13. Behavior of wind turbine efficiency.

The efficiency behavior with respect to the angular speed of the electric generator η_g , the rectifier bridge ($\eta(g + rb)$) and the overall system ($\eta(WT)$) are shown in Fig. 13. The maximum efficiency of the wind turbine was 35% and 32% under nominal conditions.

5. Conclusions

In this work it was proved the effectiveness of the methodology described for a successful coupling of the components of the small capacity wind turbines. The error between the theoretical and the experimental curves of the wind turbine performance obtained with this methodology are smaller than those reported before. Then it was demonstrated that the losses considered in this work determine the precision in the prediction of the maximum efficiency points of each wind turbine components and therefore this contributes to increase the accuracy on their coupling and the system efficiency. The results obtained with this methodology also proved its usefulness as a tool to understand the wind energy conversion in electrical energy through a PMSG.

Declarations

Author contribution statement

A. Verde: Performed the experiments; Wrote the paper.

O. Lastres: Conceived and designed the experiments.

G. Hernández, G.Ibañez: Analyzed and interpreted the data.

L. Verea: Performed the experiments.

P. Sebastian: Contributed reagents, materials, analysis tools or data.

Funding statement

This research did not receive any specific grant from funding agencies in the public, commercial, or not-for-profit sectors.

Competing interest statement

The authors declare no conflict of interest.

Additional information

No additional information is available for this paper.

References

- [1] N. Salih, A. Mohammed, A. Talha, A. Kamel, Experimental and theoretical investigation of micro wind turbine for low wind speed regions, *Renew. Energy* 116 (2018) 215–223.
- [2] H. Gitano-Briggs, *Low Speed Wind Turbine Design*, InTech, 2012 (Chapter 11).
- [3] R. Boraci, C. Vasar, Experimental applications of a pragmatic method to design control strategy for low power wind energy conversion system, *Soft Comput. Appl.* (2013) 183–195.
- [4] H. Gitano-Briggs, *Small Wind Turbine Power Controllers*, InTech, 2010 (Chapter 7).
- [5] C. Junfei, W. Hongbin, S. Ming, J. Weinan, C. Liang, G. Caiyun, Modeling and simulation of directly driven wind turbine with permanent magnet synchronous generator, in: *IEEE PES Innovative Smart Grid Technologies*, 2012.
- [6] K. Pope, R. Milman, G. Naterer, Rotor dynamics correlation for maximum power and transient control of wind turbines, *Int. J. Energy Res.* 34 (8) (2010).
- [7] C. Aravind, R. Rajparthiban, R. Rajprasad, Y. Wong, A novel magnetic levitation assisted vertical axis wind turbine—design procedure and analysis, in: *IEEE 8th International Colloquium on Signal Processing and its Applications*, 2012.
- [8] A. Shahrukh, R. Rajprasad, R. Rajparthiban, C. Aravind, Performance analysis of 20 pole 1.5 KW three phase permanent magnet synchronous generator for low speed vertical axis wind turbine, *Energy Power Eng.* 5 (2013) 423–428.

- [9] T. Porselvi, Study of Multilevel Inverter Based Wind Electric System with a Single DC Source, Faculty of Electrical Engineering, Anna University, October, 2015.
- [10] S.J. Chapman, *Electric Machinery Fundamentals*, fifth ed., McGraw-Hill, 2012.
- [11] M.J. Fraile, *Máquinas Eléctricas*, 6a Edición, McGraw-Hill, 2008.
- [12] Y. Zhu, M. Cheng, W. Hua, W. Wang, A novel maximum power point tracking control for permanent magnet direct drive wind energy conversion systems, *Energies* 5 (12) (2012) 1398–1412.
- [13] A.M. EL-Refaie, Fractional-slot concentrated-windings synchronous permanent magnet machines. Opportunities and challenges, *IEEE Trans. Ind. Electron.* 57 (1) (2010) 107–121.
- [14] O. Danielsson, M. Eriksson, M. Leijon, Study of a longitudinal flux permanent magnet linear generator for wave energy converters, *Int. J. Energy Res.* 30 (2006) 1130–1145.
- [15] M.S. Shoda, R. Chandra, S. Rana, Optimum size of base load generators for growing demand, *Int. J. Energy Res.* 18 (1994) 345–357.
- [16] A. Solum, M. Leijon, Investigating the overload capacity of a direct-driven synchronous permanent magnet wind turbine generator designed using high-voltage cable technology, *Int. J. Energy Res.* 31 (2007) 1076–1086.
- [17] J. Martinez, A. Morales, O. Probst, A. Llamas, C. Rodriguez, Analysis and simulation of a wind-electric battery charging system, *Int. J. Energy Res.* 30 (2006) 633–646.
- [18] A. Rodríguez, D. Burgos, G. Arnalte, *Sistemas eólicos de producción de energía eléctrica*, Editorial Rueda, S.L., Madrid, 2003.
- [19] K. Chungun, G. Yonghao, C. Chung, A coordinated LVRT control for a PMSG wind turbine, *IFAC Papers On Line* 50 (1) (2017) 8758–8763.
- [20] Nima Madani. Design of a Permanent Magnet Synchronous Generator for a Vertical Axis Wind Turbine. Stockholm, Sweden. XR-EE-EME 2011:013.
- [21] R. Melício, V.M.F. Mendes, J.P.S. Catalao, Modeling and simulation of wind energy systems with matrix and multilevel power converters, *IEEE Lat. Am. Trans.* 7 (1) (2009) 78–84.
- [22] M. Little, K. Pope, Performance modeling for wind turbines operating in harsh conditions, *Int. J. Energy Res.* 41 (3) (2017) 417–428.

- [23] S.M. Dehghan, M. Mohamadian, A.Y. Varjani, A new variable-speed wind energy conversion system using permanent-magnet synchronous generator and Z-source inverter, *IEEE Trans. Energy Convers.* 24 (2009) 714–724.
- [24] J.F. Gieras, R.J. Wang, M.J. Kamper, *Axial Flux Permanent Magnet Brushless Machines*, second ed., Springer, 2008.
- [25] M. Andrew, E. Glenn, Simple wind energy controller for an expanded operating range, *IEEE Trans. Energy Convers.* 20 (2) (JUNE 2005).
- [26] D. Menad, B. Jérôme, E. Ahmed, Control of wind conversion system used in autonomous system, *Energy Proc.* 62 (2014) 482–491.
- [27] A. Mohammadali, H. Arash, S. Saeideh, S. Farid, Effects of permanent magnet synchronous generator and wind turbine parameters on the performance of a small-scale wind power generation system, *Przeglad Elektrotechniczny* 87 (10) (2011).
- [28] J. Haibo, L. Yanru, C. Zhongqing, Performances of ideal wind turbine, *Renew. Energy* 83 (2015) 658–662.
- [29] T. Abhishiktha, K. Ratna, K. Dipankur, V. Indrajaya, K. Hari, A review on small-scale wind turbines, *Renew. Sustain. Energy Rev.* 56 (2016) 1351–1371.
- [30] N.A. Ahmed, A novel small-scale efficient wind turbine for power generation, *Renew. Energy* 57 (2013) 79–85.
- [31] B. Jakub, D. Krzysztof, K. Krzysztof, K. Marcin, M. Jerzy, Investigation of parameters influencing the efficiency of small wind turbines, *J. Wind Eng. Ind. Aero Dyn.* 146 (2015) 29–38.
- [32] S. Lorenzo, B. Nicola, C. Francesco, A. David, G. Alberto, Optimizing the design of horizontal-axis small wind turbines: from the laboratory to market, *J. Wind Eng. Ind. Aero Dyn.* 154 (2016) 58–68.
- [33] R. Jerson, H. David, B. Debanik, F. Erb, Drivetrain resistance and starting performance of a small wind turbine, *Renew. Energy* 117 (2018) 509–519.
- [34] C. Ciaran, B. Raymond, L. William, O. Fergal, Performance characterization of a commercial-scale wind turbine operating in an urban environment, using real data, *Energy Sustain. Dev.* 36 (2017) 44–54.
- [35] F. Matteo, M. Giovanni, D. Antonino, J. Andrew, Evaluation of surface-mounted PMSG performances connected to a diode rectifier, *IEEE Trans. Energy Convers.* (2015).

- [36] C. Huynh, L.P. ZHENG, D. Acharya, Losses in high-speed permanent magnet machines used in microturbine applications, *J. Eng. Gas Turbines Power* 131 (2009) 22301–22306.
- [37] S. Heier, *Grid Integration of Wind Energy Conversion Systems*, John Wiley & Sons Ltd, New York, USA, 1998.
- [38] R.S. Bajpai, M. Goyal, R. Gupta, Modeling and control of variable speed wind turbine using laboratory simulator, *J. Renew. Sustain. Energy* 7 (2015), 053127-19.
- [39] F. Leonardi, T. Matsuo, T.A. Lipo, Iron loss calculation for synchronous reluctance machines, *Wisconsin Power Electronics Center, Research Report* 1 (1996) 307–312.